Physical properties of mixed TiO_2-CdO thin films for gas sensor applications

H. S. Ali[a], H. R. Abd Ali[a], N. F. Habubi[a,*]
[a]*Department of Physics- College of Education for Pure Sciences-University of Tikrit, Iraq*
[b]*Department of Radiation and Sonar Technologies, Alnukhba University College, Baghdad-Iraq*

TiO_2-CdO thin films were grown by Nd: YAG pulsed laser deposition (PLD) at different laser energies of (500-900) mJ. According to the findings of the XRD analysis, each film possessed a cubic polycrystalline crystal structure with a predominant peak along the (111) plane. The average crystallite size was corrected using Warren-Scherrer's corrections, and their values were found to lie between (12.23 and 83.40) nm. The AFM images indicate that the average particle size reduced as the laser energy increased, while surface roughness and root mean square values were raised as the laser energy increased. Optical properties showed that the bandgap decreases from 2.09- 1.8 eV with increasing laser energy. The increment in laser energy results in a rise in particle size and the average roughness. The maximum Sensitivity of TiO_2-CdO films towards H_2 gas was 72.3%, and the response time was within 24– 67.9 sec.

(Received September 21, 2023; Accepted January 25, 2024)

Keywords: PLD , XRD, TiO_2-CdO, AFM, Sensor

1. Introduction

In the last decades, there has been a significant rise in scientific curiosity about metal oxides. [1]. They are essential in the glass, ceramic, and glass coatings and the manufacture of solar cells, capacitors, rectifiers, filters, transistors, detectors [2], and countless fields. Since their electrical, electronic, and optical properties may be tuned, metal-oxide thin films find widespread application in various technologies, including solar cells, photodetectors, LEDs, gas sensors, and display technologies [3-9]. TCOs, including In_2O_3, ZnO, SnO_2, and CdO, have been the subject of research by several researchers due to the possible applications of these compounds [10,11]. TCO's CdO is the first material to have a broadband gap and unique usage in flat electronic displays, LEDs, power windows, and solar devices [12,13]. These characteristics make it stand out among the other metal oxides. Anatase, brookite, and Rutile are the three various types of crystalline structures that can be observed for TiO_2 [14]. Brookite crystallizes in the orthorhombic system [15], with an energy gap of 3.20 eV for Rutile and 3.14 eV for brookite. The transformation of Anatase into Rutile occurs very slowly once the temperature is maintained at room temperature. For this phase transition, which involves a solid-state diffusion of atoms in nucleation and crystalline development [17,18], temperatures higher than 600 degrees Celsius, depending on the pressure, must be present to promote it. The fact that Anatase has a lower surface energy than Rutile allows its formation at lower temperatures. The Rutile phase can be obtained via temperatures of higher magnitude [19,20]. There is a lack of consensus in the scientific literature on the relative stability of brookite and Anatase, which is most likely dependent on the initial size of the particles that make up each compound [21]. This research aims to study the physical characterization of nanostructured TiO_2-CdO to use this mixed oxide for H_2 sensing.

* Corresponding author: n.fadhil@alnukhba.edu.iq
https://doi.org/10.15251/DJNB.2024.191.177

2. Experimental

Samples were made of high-purity Cadmium oxide (CdO) powder (99.99%) and manufactured by (Gletham Life Sciences UK), with weight ratios for (1:1) of Titanium oxide (TiO_2) powder used from the (BDH UK), with a purity of (99.8%). The mixing method was used to obtain high homogeneity between samples. After that, a hydraulic press with a press force of (6 tons) to make tablets. The Nd: YAG pulsed laser, which had a wavelength of 1064 nm, was utilized to deposit thin films, which were then employed as an energy source at a frequency of (6 Hz), and different energy (500,700,900) mJ were set to the target. The glass slides were used as bases and ultrasonically cleaned, and the distance between the target and the glass base was maintained at (4cm). The chamber was first evacuated to a pressure of (10^{-2}) mbar employing a molecular turbopump at room temperature. AFM was employed to gain film topographic nature. In contrast, SEM was utilized to get the film topography, and XRD was used to determine the crystalline structure. For the gas sensor, the test was performed at various concentrations sensing for Hydrogen (H_2) gas.

3. Results and discussions

3.1. Structural properties

The XRD patterns of TiO_2-CdO films at various energies are depicted in Figure 2. It is shown that these patterns contain peaks that are centered at 2θ= (32.727, 38.045, 55.099) and that they belong to [(111), (002), (121)] planes, respectively. The intended films were cubic polycrystalline structures with a dominance peak of (111). The dominant phase of Antase is (121) at an angle of (55,099°), which makes it the plane with the preferential direction of crystal growth, where the diffraction intensity is as high as possible. These results agree well with Zargar [22]. The crystallinity was determined through the use of equation (1). It was observed that raising the energy led to a rise in the peak intensity while also modifying the angles to higher values for 2θ. This was unexpectedly found. In addition, elevating the energy led to an accelerated rate of crystallization [23], as seen in (Table 1).

The grain size (D) was obtained utilizing Scherrer's equation [24—26].

$$G= 0.94\,\lambda / \beta\cos\theta \qquad (1)$$

where λ is XRD wavelength, β is FWHM, and θ is Bragg's angle.

The relationships listed below can be used to demonstrate how to calculate average grain size by employing Warren-Scherrer's (correction method. [27-29]

$$\beta_f = \beta_s - \beta_i \qquad \text{(Lorentzian(L) distribution)} \qquad (2)$$

$$\beta_f = \beta_s^2 - \beta_i^2 \qquad \text{(Gaussian (G) distribution)} \qquad (3)$$

Here β_f , β_s , β_i , are full widths at half maximum (FWHM) for observed, specimen, and instrumental profile functions.

The results are displayed in Table 2. The average grain size increases as the laser energy rises, showing enhancement in crystal nucleation.

The Dislocation density (δ) of intended films was evaluated by equation 4 [30-32]:

$$\varepsilon = \frac{\beta cos\theta}{4} \qquad (4)$$

The microstrain (ε) of intended films was evaluated by equation 5 [33-35]:

$$\delta = \frac{1}{D^2} \quad (5)$$

As seen in Table 1, the lattice strain decreases as the laser energy rises. CdO thin films have a higher lattice strain than TiO_2 films. The dislocation density displays the exact microstrain property

Table 1. XRD information of the intended films.

Laser energy (mj)	sample	2θ°	FWHM (degrees)	hkl	G.S (nm)	L (nm)	G (nm)	ε x 10^{-3}	δ 1/(nm^{2})
500	CdO	32.727	0.680	111	12.18	14.45	12.32	2.731	0.081
	TiO_2	55.099	0.711	121	11.60	13.30	11.71	2.749	0.085
700	CdO	32.765	0.223	111	39.46	66.00	44.41	0.933	0.023
	TiO_2	55.068	0.185	121	48.53	102.50	57.23	0.714	0.017
900	CdO	33.166	0.215	111	38.60	72.00	43.51	0.899	0.023
	TiO_2	55.068	0.145	121	61.78	188.02	83.40	0.560	0.012

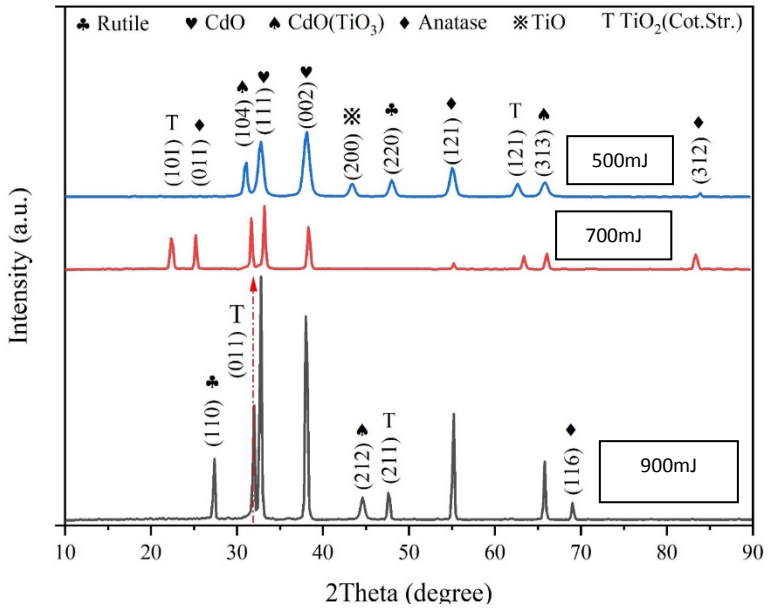

Fig. 1. XRD styles of the intended films.

3.2. EDX analysis

The energy dispersive spectroscopy (EDS) and elemental mapping studies were done to validate the appropriate range of laser energies for TiO_2-CdO thin films. Figure 2 displays the EDX spectrum and important SEM images of a 1:1 TiO_2 and CdO sample mixture. The surface morphology becomes more consistent when the laser power (P_{la}) increases. With an increase in P_{la} across the surface, it is noticed that the hole and pit that were growing on the surface have disappeared. The crystallite size increases when the P_{la} increases, and the defect density significantly reduces. After conducting these analyses, it is clear that the Cd, O, and Ti are all distributed evenly across the matrix[36,37].

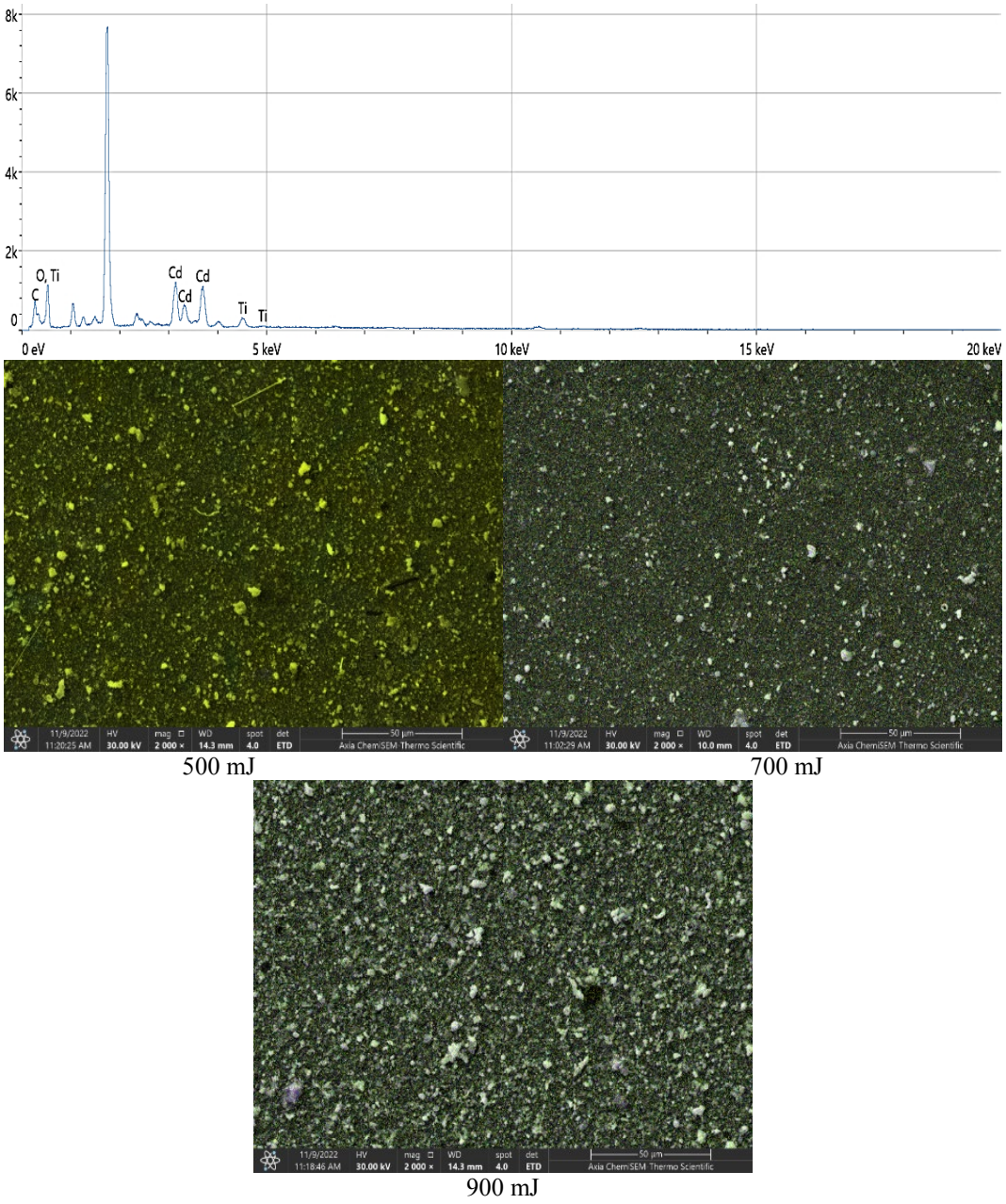

Fig. 2. EDX and mapping images from SEM.

3.3. AFM measurements

The results of the AFM measurements, average diameter (D_{av}), root mean square (rms), and average roughness (R_a)) for TiO_2 -CdO films are presented in Table 2. It was indicated that the diameter of the particle rose along with the increment in laser power due to two factors. The first reason for this event is that a rise in laser power led to the formation of larger particles. The second reason is that the increase in the laser power resulted in the growth of the grains. The energy causes the small grains to coalesce; thus, the welding process takes place, resulting in large grains, and hence, the surface roughness and grain diameter increase [38, 39]. Fig.(3) shows (AFM) images and the Granularity distributed curve of TiO_2-CdO thin films with various energies.

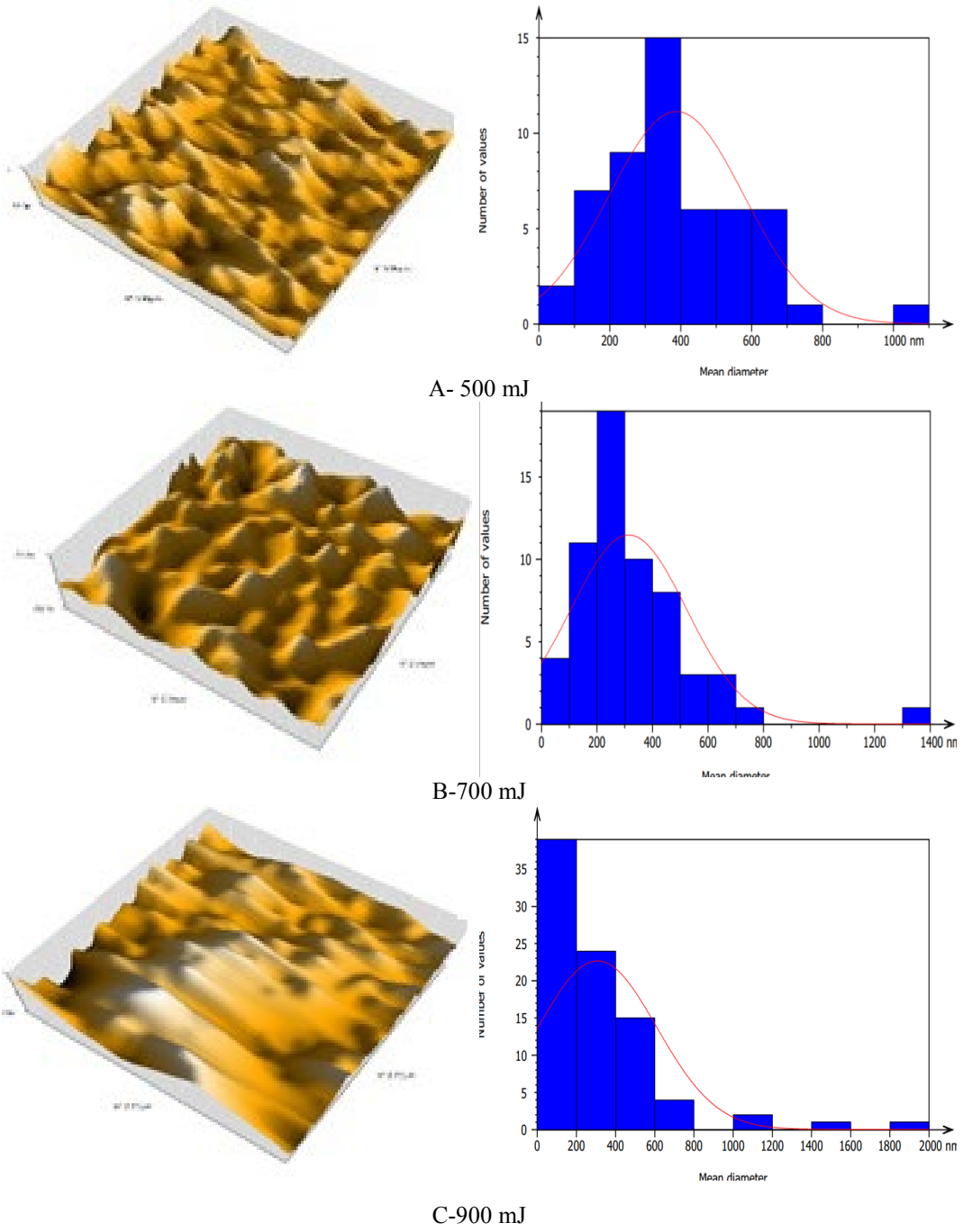

Fig. 3. AFM images and Granularity distributed curve of entended films.

Table 2. AFM parameters of the intended films.

Laser Energy (mJ)	D_{av}	rms(nm)	R_a (nm)
500	262.7	51.98	40.76
700	307.1	69.33	45.27
900	314.3	74.78	53.65

3.4. Optical properties

The optical properties of intended films were evaluated by UV–VIS spectrophotometer. The absorption coefficient (α) was calculated via Eq. (6) [40-42].

$$\alpha = 2.303\ A / t \quad (6)$$

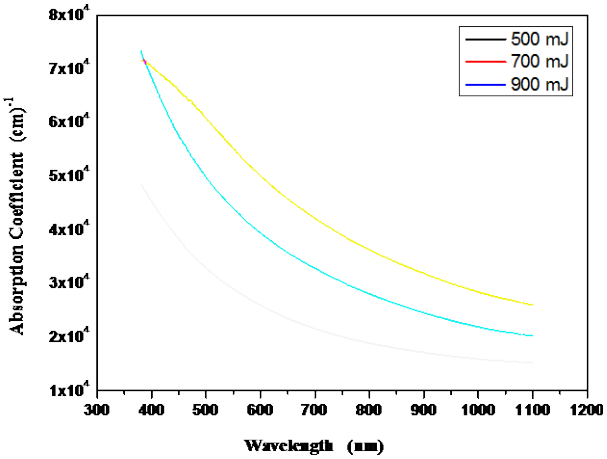

Fig. 4. α variation of the intended films.

Table 3. E_g of grown films.

Laser energy(mJ)	Eg(eV)
500	2.35
700	1.70
900	1.65

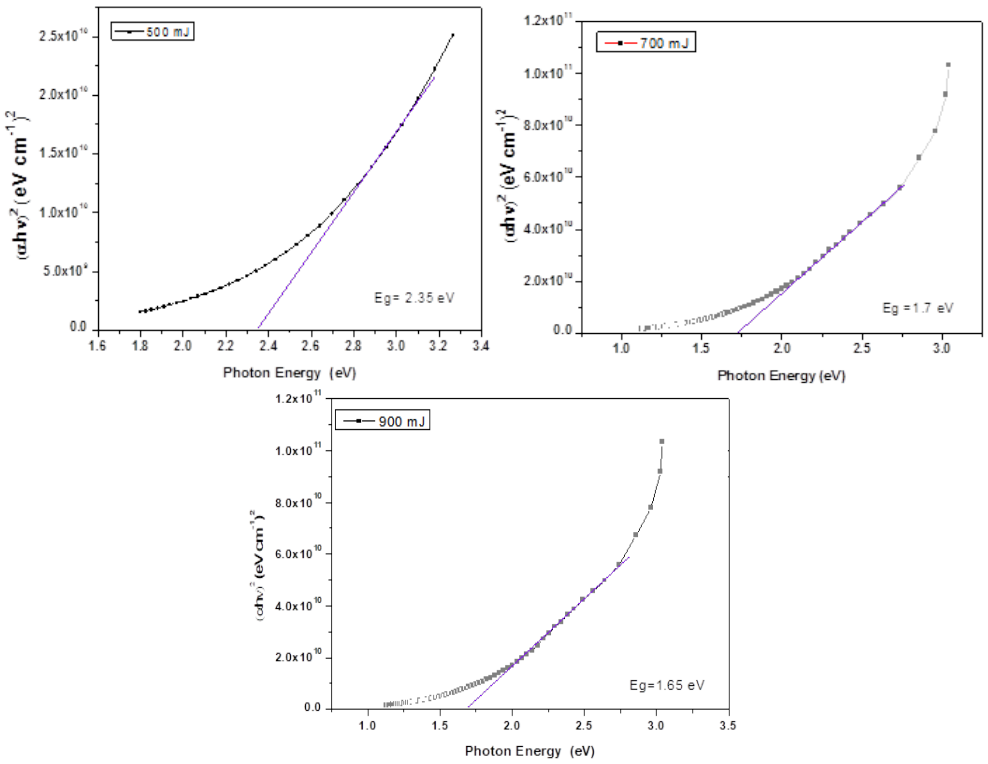

Fig. 5. Energy gap of the intended films.

The relationship between α and the wavelength in the area of (300-1100) nm is illustrated in Fig 4. It was found that α rises when the laser energy of the (TiO_2-CdO) thin films rises, which causes a rise in the probability of direct transition occurring between valence and conduction bands. The generation of donor levels within the forbidden energy gap and the conduction band is why the rise in α occurs with increasing wavelength [43-45].

The energy gap (E_g) of the intended films is shown in Fig.(5). The value of E_g is seen to decrease as the laser energy increases, as listed in Table (3), which leads to the production of localized levels close to the conduction band. This is the outcome of the formation of localized levels. As a result, a rise in the laser's intensity results in a more extraordinary level of photon absorption [46-48].

3.5. Gas sensor

The measurements were made at room temperature, using different concentrations of Hydrogen gas (H_2) prepared in the laboratory. The selection of the concentration of the appropriate amount of gas for the operation depends on obtaining the maximum response detected by the sensor for gas molecules (H_2), where the reaction energy is activated at that amount. The sensor's effectiveness largely depends on the response time, which is an essential element. The faster the response, the more efficient the sensor[49,50]. From the results obtained, the response time was within the range (24-67.9 seconds) for the thin films in Table (4). The Sensitivity was calculated for all the thin films, as it was found that the maximum Sensitivity reached (72.3%) at a concentration of (105 ppm) at an energy 900 mJ (Figure 6) [51].

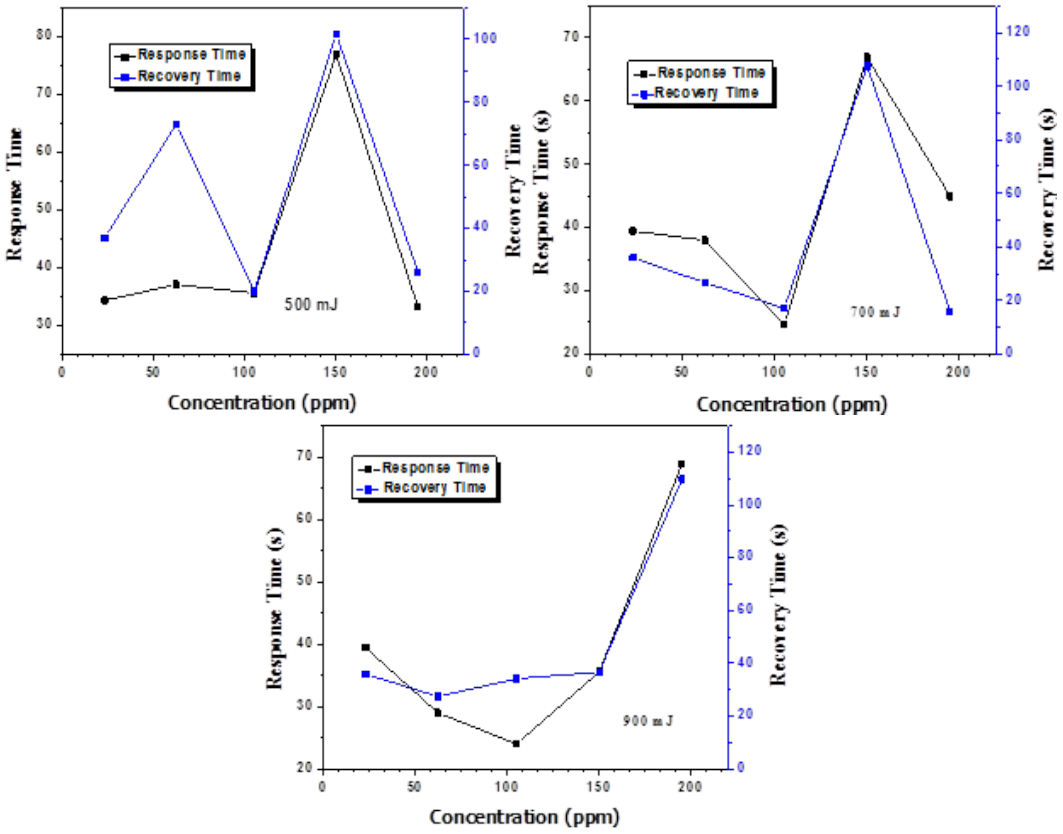

Fig. 6. Response time and recovery time versus concentration.

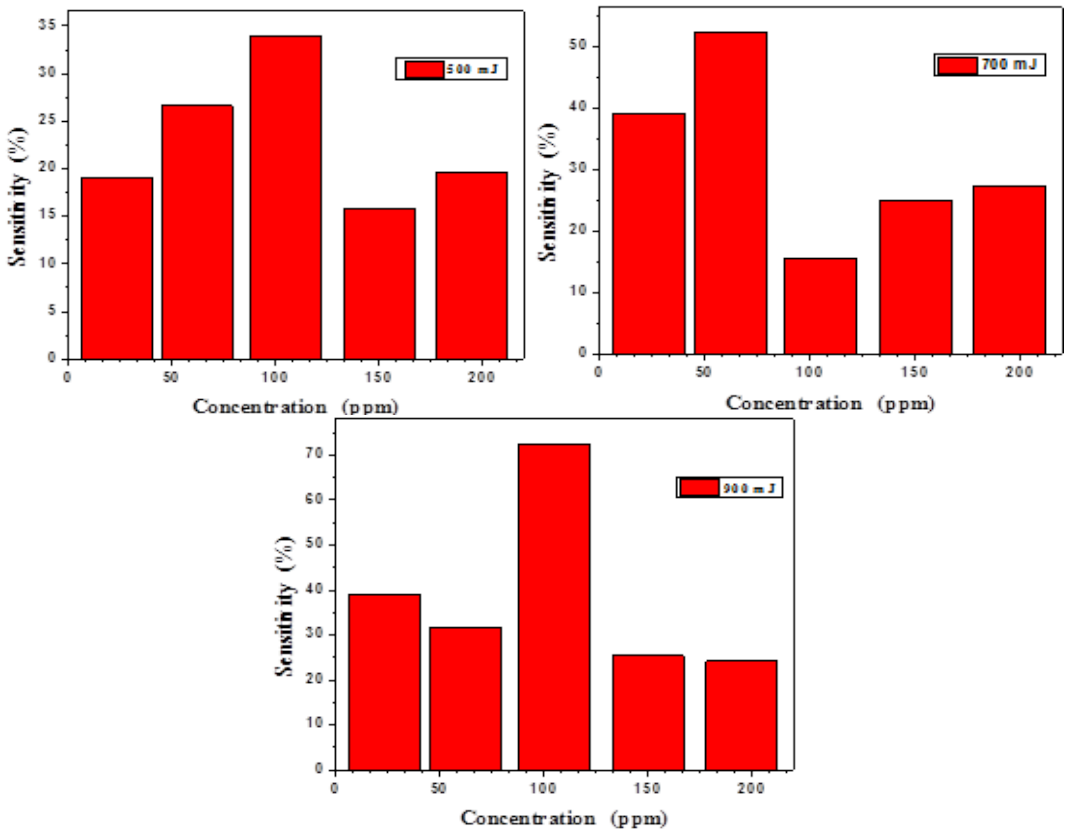

Fig .7. Sensitivity as a function of the change in the gas concentration of TiO_2-CdO thin films.

4. Conclusions

Using pulsed laser deposition (PLD), thin films of TiO_2-CdO have been produced and deposited onto a glass substrate. According to the findings of the X-rays, every single thin film was composed of polycrystalline material and had a cubic structure with a dominant direction (111). AFM results offered an increase in the diameters and roughness average, in addition to the root mean square, with a laser energy increase. It was discovered that the absorption coefficient grows as the laser energy does, which was found in contrast to the fact that the energy gap shrinks as the laser energy rises. These promising results for sensitive films TiO_2-CdO assure the use of this compound as a gas sensor.

References

[1] J. M. Martínez-Duart, R. J. Martín-Palma and F. Agulló-Rueda,"Nanotechnology for Microelectronics and Optoelectronic", Elsevier USA, (2006).
[2] H. E. Schaefer, "Nanoscience ", Springer-Verlag Berlin Heidelberg (2010).
[3] J.A. Anna Selvan, A.E. Delahoy, S. Guo, Y.-M. Li, Sol. Energy Mater. Sol. Cells. 90 , 3371-3376 (2006); https://doi: 10.1016/j.solmat.2005.09.018
[4] B.G. Lewis, D.C. Paine, MRS Bull. 25 , 22–27(2000); https://doi.org/10.1557/mrs2000.147.
[5] N. F. Habubi, R. A.Ismail , W. K. Hamoudi and H. R. Abid , Surface Review and Letters, 22(1)1550027 (8 pages))(2015). https://doi.org/10.1142/S0218625X15500274
[6] J. M. Rzaij , I. A. Ibrahim, M. A. Alalousi , and N. F. Habubi, Optik 172, 117-126 (2018); https://doi.org/10.1016/j.ijleo.2018.07.023.

[7] H. S. Mahmood, N. F. Habubi, Applied Physics A, 128 ,956-6 (2022); https://doi.org/10.1007/s00339-022-06107-6.
[8] H. R. Abed, A. M. Alwan, A. A. Yousif,and N. F. Habubi, Optical and Quantum Electronics, 51, 333 (2022); https://doi.org/10.1007/s11082-019-2046-y.
[9] E. H. Hadi, D. A. Sabur, S. S. Chiad, N. F. Habubi, K., Abass, Journal of Green Engineering, 10 (10), 8390-8400 (2020); https://doi.org/10.1063/5.0095169
[10] A. Klein, C. Korber, A. Wachau, F. Sauberlich, Y. Gassenbauer, S.P. Harvey, D.E. Proffit, T.O. Mason, Materials 3(11) , 4892– 4914 (2010); https://doi.org/10.3390/ma3114892.
[11]T.O.L. Sunde, E. Garskaite, B. Otter, H.E. Fossheim, R. Sæterli, R. Holmestad, M.-A. Einarsrud, T. Grande, J. Mater. Chem. 22, 15740–15749 (2012); .https://doi.org/10.1039/C2JM32000B.
[12] H. Shokri Kojori, J.-H. Yun, Y. Paik, J. Kim, W.A. Anderson, S.J. Kim, Nano Lett. 16, 250–254 (2016); https://doi.org//10.1021/acs.nanolett.5b03625.
[13] H. Im, H. Shao, Y.I. Park, V.M. Peterson, C.M. Castro, R. Weissleder, H. Lee, Nat. Biotechnol. 32, 490–495 (2014); https://doi.org/10.1038/nbt.2886
[14] A. Yamakata, J.J.M. Vequizo, J. Photochem. Photobiol. C Photochem. Rev. 40 , 234(2019). https://doi.org/10.1016/j.jphotochemrev.2018.12.001.
[15] T.R. Esch, I. Gadaczek, T. Bredow, Appl. Surf. Sci. 288 , 275(2014); http://dx.doi.org/10.1016/j.apsusc.2013.10.021.
[16] E. Zhang, Y. Pan, T. Lu, Y. Zhu, W. Dai, Appl. Phys. A 126 606 (2020); https://doi.org/10.1063/1.5107484.
[17] D. Zhang, S. Dong, Prog. Nat. Sci. Mater. Int. 29 ,277 (2019); https://doi.org/10.1016/j.pnsc.2019.03.012.
[18] C.G. Ezema, A.C. Nwanya, B.E. Ezema, M. Maaza, P.O. Ukoha, F.I. Ezema, J. Solid State Electrochem. 21 ,2655(2017); https://doi.org/10.1007/s10008-017-3652-x
[19] M. Cargnello, T.R. Gordon, C.B. Murray, Chem. Rev. 114 ,9319 (2014); https://doi.org/10.1021/cr500170p.
[20] Y. Wang, L. Zhang, K. Deng, X. Chen, Z. Zou, J. Phys. Chem. C 111,2709 (2007); https://doi.org/10.1021/jp066519k
[21] O. Carp, C.L. Huisman, A. Reller, Prog. Solid State Chem. 32 , 33 (2004); http://dx.doi.org/10.1016/j.progsolidstchem.2004.08.001
[22] R. A. Zargar, Materials Letters, 335, 133813 (2023); https://doi.org/10.1016/j.matlet.2022.133813.
[23] Z. Zhao, D. L., Morel, C. S. Ferekides, Thin Solid Films, 413 (1-2) , 203- 211(2002); https://doi.org/10.1016/S0040-6090(02)00344-9
[24] N. Y. Ahmed, B. A. Bader, M. Y. Slewa, N. F. Habubi, S. S. Chiad, NeuroQuantology, 18(6), 55-60 (2020); https://doi.org/10.1016/j.jlumin.2021.118221
[25] S. S. Chiad, H. A. Noor, O. M. Abdulmunem, N. F. Habubi, M. Jadan, J. S. Addasi, Journal of Ovonic Research, 16 (1), 35-40 (2020).
[26] H. T. Salloom, E. H. Hadi, N. F. Habubi, S. S. Chiad, M. Jadan, J. S. Addasi, Digest Journal of Nanomaterials and Biostructures, 15 (4), 189-1195 (2020); https://doi.org/10.15251/DJNB.2020.154.1189
[27] H. A. Hussin, R. S. Al-Hasnawy, R. I. Jasim, N. F. Habubi, S. S. Chiad, Journal of Green Engineering, 10(9), 7018-7028 (2020); https://doi.org/10.1088/1742-6596/1999/1/012063
[28] S. S Chiad,, A. S. Alkelaby, K. S. Sharba,, Journal of Global Pharma Technology, 11 (7), 662-665, (2020); https://doi.org/10.1021/acscatal.1c01666
[29] R. S Ali, N. A. H. Al Aaraji, E. H. Hadi, N. F. Habubi, S. S. Chiad, Journal of Nanostructures,10(4), 810–816 (2020); https://doi: 10.22052/jns.2020.04.014
[30] A. A. Khadayeir, R. I. Jasim, S. H. Jumaah, N. F, Habubi, S. S. Chiad, Journal of Physics: Conference Series,1664 (1) (2020); https://doi.org/10.1088/1742-6596/1664/1/012009
[31] Chiad, S.S., Noor, H.A., Abdulmunem, O.M., Habubi, N.F., Journal of Physics: Conference Series 1362(1), 012115 (2019); https://doi.org/10.1088/1742-6596/1362/1/012115

[32] A. S. Al Rawas, M. Y. Slewa, B. A. Bader, N. F. Habubi, S. S. Chiad, Journal of Green Engineering,10 (9), 7141-7153 (2020); https://doi.org/10.1021/acsami.1c00304
[33] R. S. Ali, M. K. Mohammed, A. A. Khadayeir, Z. M. Abood, N. F. Habubi and S. S. Chiad, Journal of Physics: Conference Series, 1664 (1), 012016 (2020); https://doi:10.1088/1742-6596/1664/1/012016
[34] K. Y. Qader, R. . Ghazi, A. M. Jabbar, K. H. Abass, S. S. Chiad, Journal of Green Engineering, 10 (10), 7387-7398, 2020. https://doi.org/10.1016/j.jece.2020.104011
[35] R. S. Ali, H. S. Rasheed, N. F. Habubi, S.S. Chiad, Chalcogenide Letters, 20 (1), 63–72 (2023; https://doi.org/10.15251/CL.2023.201.6
[36] A. Ghazai, K. Qader, N. F. Hbubi, S. S. Chiad, O. Abdulmunem, IOP Conference Series: Materials Science and Engineering, 870 (1), 012027 (2020); https://doi.org/ 10.1088/1757-899X/870/1/012027
[37] B. A. Bader, S. K. Muhammad, A. M. Jabbar, K. H. Abass, S. S. Chiad, N. F. Habubi, J. Nanostruct, 10 (4): 744-750, (2020); https://doi.org/ 10.22052/JNS.2020.04.007
[38] Z. Wu, D. Yuan, S. Lin, W. Guo, D. Zhan, L. Sun, C. Lin,. Int. J. Hydrog. Energy, 45, 32012-32021 (2020); https://doi.org/10.1016/j.ijhydene.2020.08.258.
[39] E. S. Hassan, K. Y. Qader, E. H. Hadi, S. S. Chiad, N. F. Habubi, K. H. Abass, Nano Biomedicine and Engineering, 12(3), pp. 205-213 (2020); https://doi.org/10.5101/nbe.v12i3.p205-213
[40] M.O. Dawood, S.S. Chiad, A.J. Ghazai, N.F. Habubi, O.M. Abdulmunem, AIP Conference Proceedings 2213, 020102,(2020); https://doi.org/10.1063/5.0000136
[41] A. A. Khadayeir, E. S. Hassan, S. S. Chiad, N. F. Habubi, K. H. Abass, M. H. Rahid, T. H. Mubarak, M. O. Dawod, and I.A. Al-Baidhany, Journal of Physics: Conference Series 1234 (1), 012014, (2019); https://doi.1088/1742-6596/1234/1/012014
[42] Hassan, E.S., Mubarak, T.H., Chiad, S.S., Habubi, N.F., Khadayeir, A.A., Dawood, M.O., Al-Baidhany, I. A. , Journal of Physics: Conference Series, 1294(2), 022008 (2019); https://doi.1088/1742-6596/1294/2/022008
[43] T. Asanuma, T. Matsutani, C. Liu, T. Mihara, M. Kiuchi, Journal of Applied Physics, 95, 11 ,6011-6016(2004); https://doi.org/10.1063/1.1728313.
[44] N. Y. Ahmed, B. A. Bader, M. Y. Slewa, N. F. Habubi, S. S. Chiad, NeuroQuantology, 18(6), 55-60 (2020); https://doi.org/10.14704/nq.2020.18.6.NQ20183
[45] B. J. Zheng, J. S. Lian, L. Zhao, Q. Jiang, Vacuum, 85, 9 , 861-865(2011); https://doi.org/10.1016/j.vacuum.2011.01.002.
[46] S. S. Chiad, N. F. Habubi, W. H. Abass, M.H. Abdul-Allah, Journal of Optoelectronics and Advanced Materials, 18(9-10), 822-826, (2016).
[47] F. H. Jasim, H. R. Shakir, S. S. Chiad, N. F. Habubi, Y. H. Kadhi,, Jadan, M., Digest Journal of Nanomaterials and Biostructures, 18(4), 1385–1393 (2023); https://doi.org/10.15251/DJNB.2023.184.1385
[48] F. A. Jasima , Z. S. A. Mosa, N. F. Habubi, Y. H. Kadhim, S. S. Chiad, Digest Journal of Nanomaterials and Biostructures, 18 (3), 1039–1049 (2023); https://doi.org/10.15251/DJNB.2023.183.1039
[49] S. K. Muhammad, E. S. Hassan, K. Y. Qader, K. H. Abass, S. S. Chiad, N. F. Habubi, Nano Biomedicine and Engineering, 12 (1), pp. 67-74, (2020); https://doi.org/10.5101/nbe.v12i1.p67-74
[50] V. Sysoev, B. Button, K.Wepsoec, S .Dmitriev, A. Kolmakov, Nano Lett., 6 , 1584-1588 (2006). https://doi.org/10.1021/nl060185t.
[51] T. Asanuma, T. Matsutani, C. Liu, T. Mihara, M. Kiuchi, Journal of Applied Physics, 95 (11) 6011-6016 (2004); https://doi.org/10.1063/1.1728313.